DEUTSCHES ELEKTRONEN-SYNCHROTRON
Ein Forschungszentrum der Helmholtz-Gemeinschaft

DESY 19-173
arXiv:1910.00451
September 2019

Measurement of the Extragalactic Background Light Spectral Energy Distribution with VERITAS

VERITAS Collaboration

ISSN 0418–9833

PLATANENALLEE 6 - 15738 ZEUTHEN

DESY behält sich alle Rechte für den Fall der Schutzrechtserteilung und für die wirtschaftliche Verwertung der in diesem Bericht enthaltenen Informationen vor.

DESY reserves all rights for commercial use of information included in this report, especially in case of filing application for or grant of patents.

To be sure that your reports and preprints are promptly included in the HEP literature database send them to (if possible by air mail):

DESY	DESY
Zentralbibliothek	Bibliothek
Notkestraße 85	Platanenallee 6
22607 Hamburg	15738 Zeuthen
Germany	Germany

A

arXiv:1910.00451v1 [astro-ph.HE] 1 Oct 2019

A. U. Abeysekara,[1] A. Archer,[2] W. Benbow,[3] R. Bird,[4] A. Brill,[5] R. Brose,[6]
M. Buchovecky,[4] D. Calderon-Madera,[7] J. L. Christiansen,[8] W. Cui,[9] M. K. Daniel,[3]
A. Falcone,[10] Q. Feng,[5] M. Fernandez-Alonso,[11] J. P. Finley,[12] L. Fortson,[13] A. Furniss,[7]
A. Gent,[14] C. Giuri,[15] O. Gueta,[15] D. Hanna,[16] T. Hassan,[15] O. Hervet,[17] J. Holder,[18]
G. Hughes,[3] T. B. Humensky,[5] C. A. Johnson,[19] P. Kaaret,[20] M. Kertzman,[2] D. Kieda,[1]
M. Krause,[15] F. Krennrich,[21] S. Kumar,[16] M. J. Lang,[22] G. Maier,[15] P. Moriarty,[22]
R. Mukherjee,[23] M. Nievas-Rosillo,[15] S. O'Brien,[16] R. A. Ong,[4] K. Pfrang,[15] M. Pohl,[6]
R. R. Prado,[15] E. Pueschel,[15] J. Quinn,[24] K. Ragan,[16] P. T. Reynolds,[25] D. Ribeiro,[5]
G. T. Richards,[18] E. Roache,[3] A. C. Rovero,[11] I. Sadeh,[15] M. Santander,[26]
G. H. Sembroski,[12] K. Shahinyan,[13] I. Sushch,[27] T. Svraka,[7] A. Weinstein,[21] R. M. Wells,[21]
P. Wilcox,[20] A. Wilhelm,[6] D. A. Williams,[17] T. J Williamson,[18] and B. Zitzer[16]

[1]*Department of Physics and Astronomy, University of Utah, Salt Lake City, UT 84112, USA*

[2]*Department of Physics and Astronomy, DePauw University, Greencastle, IN 46135-0037, USA*

[3]*Center for Astrophysics Harvard & Smithsonian, Cambridge, MA 02138, USA*

[4]*Department of Physics and Astronomy, University of California, Los Angeles, CA 90095, USA*

[5]*Physics Department, Columbia University, New York, NY 10027, USA*

[6]*Institute of Physics and Astronomy, University of Potsdam, 14476 Potsdam-Golm, Germany and DESY, Platanenallee 6, 15738 Zeuthen, Germany*

[7]*Department of Physics, California State University - East Bay, Hayward, CA 94542, USA*

[8]*Physics Department, California Polytechnic State University, San Luis Obispo, CA 94307, USA*

[9]*Department of Physics and Astronomy, Purdue University, West Lafayette, IN 47907, USA and Department of Physics and Center for Astrophysics, Tsinghua University, Beijing 100084, China.*

[10]*Department of Astronomy and Astrophysics, 525 Davey Lab, Pennsylvania State University, University Park, PA 16802, USA*

[11]*Instituto de Astronoma y Fsica del Espacio (IAFE, CONICET-UBA), CC 67 - Suc. 28, (C1428ZAA) Ciudad Autnoma de Buenos Aires, Argentina*

[12]*Department of Physics and Astronomy, Purdue University, West Lafayette, IN 47907, USA*

[13]*School of Physics and Astronomy, University of Minnesota, Minneapolis, MN 55455, USA*

[14]*School of Physics and Center for Relativistic Astrophysics, Georgia Institute of Technology, 837 State Street NW, Atlanta, GA 30332-0430*

[15]*DESY, Platanenallee 6, 15738 Zeuthen, Germany*

[16]*Physics Department, McGill University, Montreal, QC H3A 2T8, Canada*

[17]*Santa Cruz Institute for Particle Physics and Department of Physics, University of California, Santa Cruz, CA 95064, USA*

[18]*Department of Physics and Astronomy and the Bartol Research Institute, University of Delaware, Newark, DE 19716, USA*

[19]*Santa Cruz Institute for Particle Physics and Department of Physics, University of California, Santa Cruz, CA 95064, USA, now at NextEra Analytics, Inc., St. Paul, MN 55107, USA*

[20]*Department of Physics and Astronomy, University of Iowa, Van Allen Hall, Iowa City, IA 52242, USA*

[21]*Department of Physics and Astronomy, Iowa State University, Ames, IA 50011, USA*

[22]*School of Physics, National University of Ireland Galway, University Road, Galway, Ireland*
[23]*Department of Physics and Astronomy, Barnard College, Columbia University, NY 10027, USA*
[24]*School of Physics, University College Dublin, Belfield, Dublin 4, Ireland*
[25]*Department of Physical Sciences, Cork Institute of Technology, Bishopstown, Cork, Ireland*
[26]*Department of Physics and Astronomy, University of Alabama, Tuscaloosa, AL 35487, USA*
[27]*Institute of Physics and Astronomy, University of Potsdam, 14476 Potsdam-Golm, Germany*

Keywords:

° ′ ″ ° ′ ″

°

°

°

wobble

1

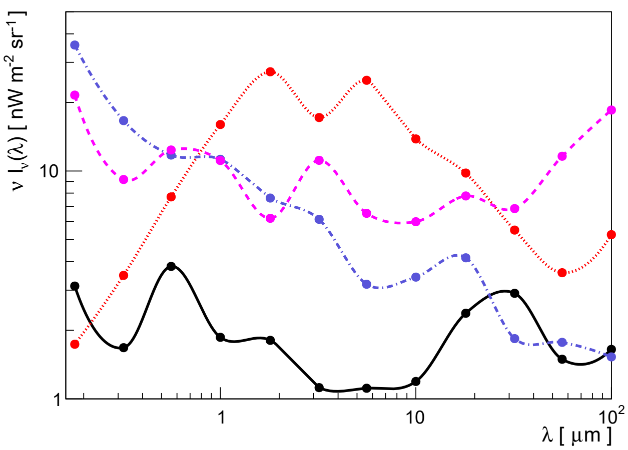
ν I_ν(λ) [nW m^-2 sr^-1]
10
1
1
10
10^2
λ [μm]

$-$ $-$

$-_{\mathrm{evo}}$

$' \; ' \quad ' \quad '$

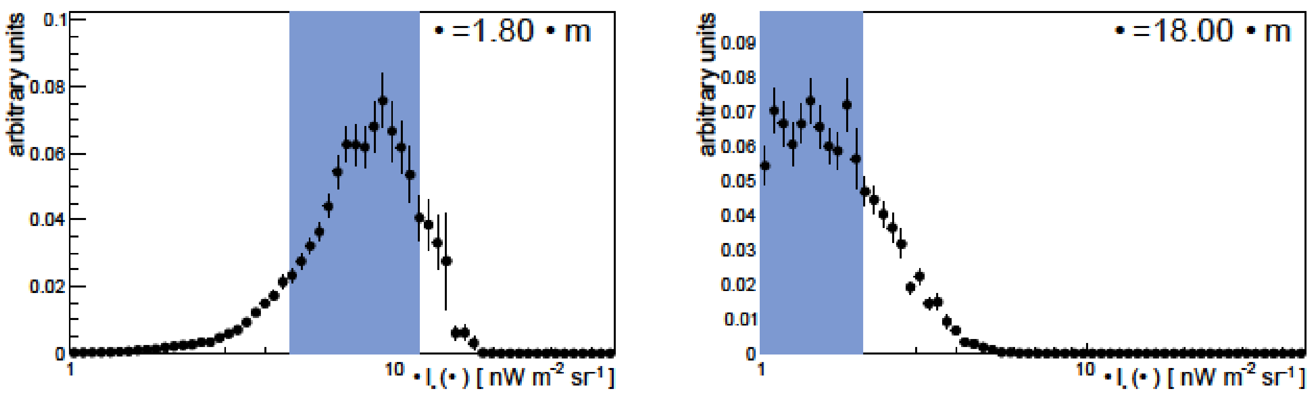

Figure 2. Example EBL intensity probability distributions. The shaded bands indicate the 68% containment bands. In the left panel, a two-sided containment band for $\nu I_\nu(\lambda)$ can be extracted, whereas in the right panel only an upper limit can be set.

wavelength range is defined by the width of the pair-production cross section after integration over the line of sight, and can be approximated as

$$\lambda_{\rm EBL} \simeq [0.5\,\mu{\rm m} - 5\,\mu{\rm m}] \times \left(\frac{E_\gamma}{1\,{\rm TeV}}\right) \times (1+z)^2, \qquad (1)$$

taking E_γ as the energy of the lowest-energy and highest-energy differential flux points in the source's photon spectrum. The highest-energy flux point is taken to be either one flux point beyond the last point with $\geq 2\sigma$ significance, or the last point with the number of source region counts >0 by 2σ, whichever point is of higher energy.

A projection of the EBL intensity probability distribution at each $\lambda_{\rm EBL}$ grid point is made. Initially a flat distribution, each EBL shape is weighted by $\exp(-\chi^2/2)$, with χ^2 taken from the fit to the EBL-corrected spectrum. This choice of weighting disfavors EBL shapes whose EBL-corrected spectra are poorly described by the physically motivated spectral models considered.

The constraints from multiple blazars are combined by weighting the EBL model by $\exp(-(\Sigma\chi^2)_n/2)$, where n is an index over the sources. It is worth noting that the spectra are produced with comparable energy binning, ensuring that sources do not receive a greater or lesser weight in the combination based on the choice of binning. At each grid point in $\lambda_{\rm EBL}$, only sources contributing according to Eq. 1 are included in the sum. Two example distributions, after χ^2 weighting, are shown in Figure 2.

A measurement of the EBL intensity is made by integrating the desired (68% or 95%) containment. As the probability distributions are in general asymmetric, the quantiles are extracted by integrating inwards from where the distribution tails to zero, rather than outward from a central value. Examples of 68% containment bands are shown by the shaded regions in Figure 2. In the right panel, only an upper limit on the EBL intensity can be set, as opposed to the left panel, where both the upper and lower tails of the probability distribution fall to zero.

The accuracy of the method is tested by taking spectra from a bright, nearby source (10 spectra derived from short observations of the Crab Nebula, where event counts are comparable to those of the EBL sources) and calculating the expected spectra at z=0.09, 0.2, 0.3, 0.4, 0.5, and 0.6 using the model of Gilmore et al. (2012). The extracted 68% containment band contains the input value of the EBL intensity for all redshifts.

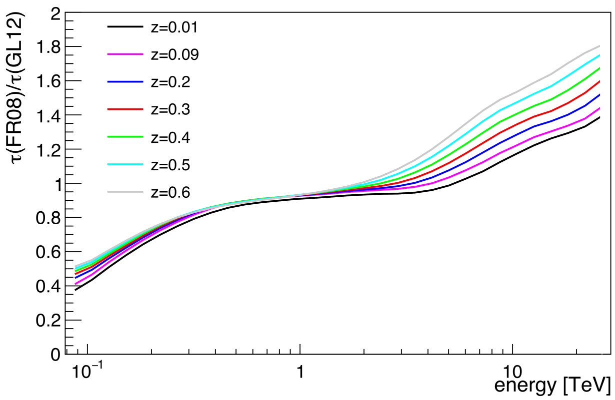

τ(FR08)/τ(GL12)
z=0.01
z=0.09
z=0.2
z=0.3
z=0.4
z=0.5
z=0.6
2
1.8
1.6
1.4
1.2
1
0.8
0.6
0.4
0.2
0
10^−1
1
10
energy [TeV]

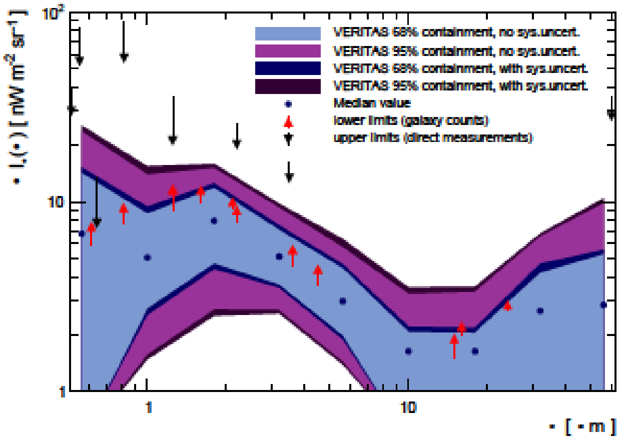

Figure 4. Measured 68% and 95% containment bands on the EBL intensity as a function of wavelength. The dark and light shaded regions illustrate the bands with and without systematic uncertainties, respectively. The filled circles mark the median values of the EBL intensity probability distributions. Upward-facing arrows show lower limits from galaxy counts, downward-facing arrows show upper limits from direct measurements.

λ [μm]	$\nu I_\nu^{\min}$(95% CI) [nW m^{-2} sr^{-1}]	$\nu I_\nu^{\min}$(68% CI) [nW m^{-2} sr^{-1}]	$\nu I_\nu^{\max}$(68% CI) [nW m^{-2} sr^{-1}]	$\nu I_\nu^{\max}$(95% CI) [nW m^{-2} sr^{-1}]
0.56	-	-	15.2	25.2
1.00	1.5	2.5	9.4	15.4
1.80	2.5	4.4	12.5	15.9
3.20	2.6	3.5	7.5	9.8
5.60	1.4	1.9	4.7	6.4
10.00	-	-	2.2	3.5
18.00	-	-	2.2	3.6
32.00	-	-	4.7	6.8
56.00	-	-	5.6	10.4

Table 5. Measured 68% and 95% containment bands on the EBL intensity as a function of EBL wavelength, including systematic uncertainties. A dash indicates that no lower limit could be set. The treatment of the redshift uncertainty for two of the sources is discussed in Section 5.

model of Gilmore et al. (2012) is included for reference. All gamma-ray measurements are consistent with each other and with Gilmore et al. (2012), which for this wavelength region is consistent with other state-of-the-art models. Taken together, these measurements point to an EBL SED that is well described by the lower limits from galaxy counts, although the uncertainties remain too large to rule out a diffuse component. It is clearly seen that the approach taken here has more power to constrain high EBL intensities than low EBL intensities, which has been remarked upon in other EBL measurements using imaging atmospheric Cherenkov telescopes (Abdalla et al. 2017; Acciari et al. 2019).

7. CONCLUSIONS

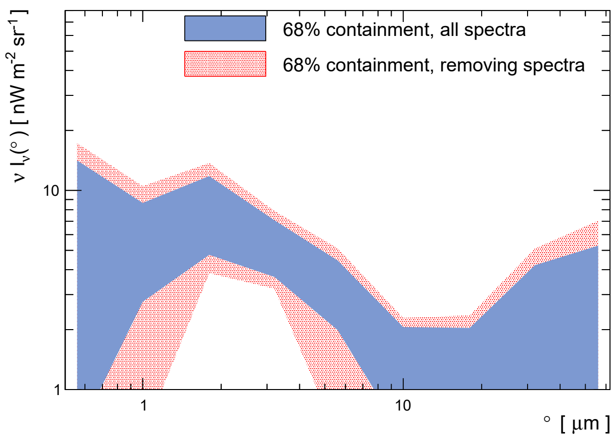

Figure 5. Measured 68% containment bands on the EBL intensity as a function of EBL wavelength, taking the most conservative bands obtained after removing the sources individually, overplotted with the 68% containment band including all spectra (without systematic uncertainties).

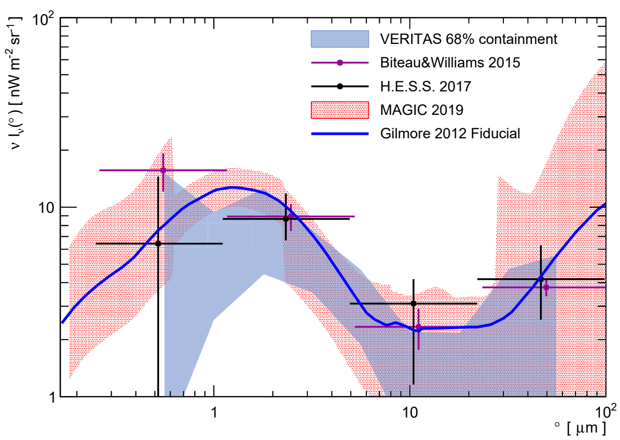

Figure 6. Measured 68% containment on the EBL intensity as a function of wavelength, compared to the recent gamma-ray measurements of Biteau & Williams (2015), H.E.S.S. (Abdalla et al. 2017), and MAGIC (Acciari et al. 2019), and the model of Gilmore et al. (2012).

Nine years of VERITAS observations of 14 hard-spectrum blazars, located from redshift z=0.044 to z=0.604, were used to extract a measurement of the EBL intensity as a function of wavelength. The approach taken made minimal assumptions about the EBL shape and evolution, and made conservative assumptions about the intrinsic spectra of blazars. No individual source is dominant in the resulting joint measurement, and the systematic uncertainties are small in comparison to the statistical uncertainties. This indicates that the VERITAS results can be improved by deeper exposures and better-measured spectra. This is particularly true at large values of λ_{EBL}, where the state-of-the-art EBL models begin to disagree in their predictions. The agreement between the extracted EBL SED and lower limits from galaxy counts indicates that most, if not all, of the EBL photons can be attributed to resolved galaxies in the wavelength range covered by this measurement. Looking beyond currently operating instruments, a more complete picture of the

Facilities: